THE JOURNAL OF BIOLOGICAL CHEMISTRY VOL. 282, NO. 26, pp. 19092–19102, June 29, 2007

Novel Role of Y1 Receptors in the Coordinated Regulation of Bone and Energy Homeostasis*

Received for publication, January 23, 2007, and in revised form, April 19, 2007 Published, JBC Papers in Press, May 9, 2007, DOI 10.1074/jbc.M700644200

Paul A. Baldock[‡1], Susan J. Allison[‡1,2], Pernilla Lundberg[§¶], Nicola J. Lee[§], Katy Slack[§], En-Ju D. Lin[§], Ronaldo F. Enriquez[‡], Michelle M. McDonald[‖], Lei Zhang[§], Matthew J. During[**], David G. Little[‖], John A. Eisman[‡], Edith M. Gardiner[‡‡3], Ernie Yulyaningsih[§], Shu Lin[§], Amanda Sainsbury[§4], and Herbert Herzog[§4,5]

From the [‡]Bone and Mineral Program and [§]Neuroscience Research Program, Garvan Institute of Medical Research, St Vincent's Hospital, 384 Victoria St, Darlinghurst, Sydney, New South Wales 2010, the [¶]Department of Oral Cell Biology, Umeå University, Umeå S-901 87, Sweden, the [‖]Department of Orthopaedic Research & Biotechnology, The Children's Hospital at Westmead, Sydney 2000, Australia, the [**]Department of Molecular Medicine & Pathology, University of Auckland, Auckland 1001, New Zealand, and the [‡‡]Diamantina Institute, University of Queensland, Princess Alexandra Hospital, Brisbane, Queensland 4102, Australia

The importance of neuropeptide Y (NPY) and Y2 receptors in the regulation of bone and energy homeostasis has recently been demonstrated. However, the contributions of the other Y receptors are less clear. Here we show that Y1 receptors are expressed on osteoblastic cells. Moreover, bone and adipose tissue mass are elevated in $Y1^{-/-}$ mice with a generalized increase in bone formation on cortical and cancellous surfaces. Importantly, the inhibitory effects of NPY on bone marrow stromal cells *in vitro* are absent in cells derived from $Y1^{-/-}$ mice, indicating a direct action of NPY on bone cells via this Y receptor. Interestingly, in contrast to Y2 receptor or germ line Y1 receptor deletion, conditional deletion of hypothalamic Y1 receptors in adult mice did not alter bone homeostasis, food intake, or adiposity. Furthermore, deletion of both Y1 and Y2 receptors did not produce additive effects in bone or adiposity. Thus Y1 receptor pathways act powerfully to inhibit bone production and adiposity by non-hypothalamic pathways, with potentially direct effects on bone tissue through a single pathway with Y2 receptors.

Many physiological functions are regulated by signals processed within the brain. Y receptors, members of the G-protein-coupled receptor superfamily, play an important role in this regulatory axis, mediated by their endogenous ligands: neuropeptide Y (NPY),[6] peptide YY, and pancreatic polypeptide. The Y receptor system is complex, consisting of five Y receptors (Y1, Y2, Y4, Y5, and y6), each with varying distributions across peripheral and central tissues, including the hypothalamus. Among a number of responsive tissues, both bone and adipose tissue are known to be regulated, at least in part, via hypothalamic Y2 receptors (1–4). Indeed, lack of central Y2 signaling, as in hypothalamus-specific Y2 receptor conditional knock-out mice, causes increased bone mass (1). Furthermore, deletion of Y2 receptors has recently been demonstrated to decrease Y1 receptor expression in stromal cells, associated with a greater population of progenitor cells, and accounting for the greater synthetic activity of these cells *in vitro* suggesting an important role of this Y receptor in bone formation as well (see the accompanying report (39).

Y1 receptors are widely expressed in the central nervous system, including the hypothalamus (5, 6), as well as on peripheral tissues such as vascular smooth muscle cells (7) and pancreatic β cells (8). Y1 receptors are expressed on bone marrow stromal cells and bone tissue (see accompanying report (39)), by contrast, Y2 receptors have not been detected on bone. In addition to effects in bone, Y1 receptors have been considered as important regulators of energy homeostasis, consistent with pharmacological evidence from Y receptor agonists and antagonists to stimulate or inhibit feeding (9). Fasting-induced re-feeding is reduced in germ line Y1 receptor knock-out mice (10), and deletion of Y1 receptors in genetically obese *ob*/*ob* mice, in which hypothalamic NPY-ergic activity is chronically increased, significantly reduces food intake and body weight (11). Paradoxically, germ line Y1 receptor knock-out mice develop late-onset obesity in the absence of hyperphagia (10, 12, 13). One hypothesis to reconcile this apparent discrepancy is that hypothalamic and non-hypothalamic Y1 receptors have different effects on energy homeostasis.

Given the clear involvement of Y1 receptors in the regulation of energy homeostasis as well as new evidence of a putative role for Y1 receptors on osteoblast-like cells, we investigated the effect of germ line and conditional (adult-onset, hypothalamus-specific) deletion of Y1 receptors in mice. In addition, the potential interaction between Y1 receptor sig-

* This work was supported by the National Health and Medical Research Council (NHMRC, Grant 376021 to H. H. and Grant 230820 to A. S.), by an NHMRC Fellowship (188827) and the Diabetes Australia Research Trust (to A. S.), by an NHMRC scholarship (to S. J. A.), an NHMRC Fellowship (to H. H.), by a Swedish Society for Medical Research fellowship (to P. L.), and by the Swedish Research Council for Medicine. The costs of publication of this article were defrayed in part by the payment of page charges. This article must therefore be hereby marked "*advertisement*" in accordance with 18 U.S.C. Section 1734 solely to indicate this fact.

[1] Both authors contributed equally to this work.
[2] Present address: Laboratory of Neural Stem Cell Biology, Stem Cell Institute, University Hospital, Lund 22184, Sweden.
[3] Present address: School of Medicine, University of Queensland, Brisbane 4000, Queensland, Australia.
[4] Both authors contributed equally to this work.
[5] To whom correspondence should be addressed: Tel.: 61-2-9295-8296; Fax: 61-2-9295-8281; E-mail: h.herzog@garvan.org.au.

[6] The abbreviations used are: NPY, neuropeptide Y; WAT, white adipose tissue; BAT, brown adipose tissue; MAR, mineral apposition rate; rAAV, adeno-associated viral vector.

naling and the previously identified Y2 receptor pathway was assessed in $Y1^{-/-}Y2^{-/-}$ double knock-out mice.

EXPERIMENTAL PROCEDURES

Animal Care—All research and animal care procedures were approved by the Garvan Institute/St. Vincent's Hospital Animal Experimentation Ethics Committee and were in agreement with the Australian Code of Practice for the Care and Use of Animals for Scientific Purpose. All mice were fed a normal chow diet *ad libitum* (6% calories from fat, 21% calories from protein, 71% calories from carbohydrate, 2.6 kilocalories/g, Gordon's Specialty Stock Feeds, Yanderra, New South Wales, Australia), with *ad libitum* access to water.

Generation of $Y1^{-/-}$ and $Y1^{-/-}Y2^{-/-}$ Double Mutant Mice—A targeting vector for the Y1 and Y2 receptor genes (*Npy1r* and *Npy2r*, respectively) has been used to produce both germ line ($Y1^{-/-}$ or $Y2^{-/-}$) and conditional (floxed, $Y1^{lox/lox}$ or $Y2^{lox/lox}$) knock-out mice, as previously published (2, 14). Both of these knock-out strategies result in deletion of the entire coding region of the Y1 or Y2 receptor, including the neomycin selection cassette. Germ line $Y1^{-/-}$ and $Y2^{-/-}$ lines were bred to generate double heterozygote mice, which were then crossed to obtain the double knock-out mouse line. All mice were on a mixed C57BL/6–129/SvJ background.

Generation of Adult-onset Hypothalamus-specific Y1 Receptor Knock-out Mice ($Y1^{Hyp}$)—9- to 10-week-old $Y1^{lox/lox}$ mice were anesthetized with 100/20 mg/kg ketamine/xylazine (Parke Davis-Pfizer, Sydney, Australia and Bayer AG, Leverkusen, Germany). With the head in the flat skull position using a stereotaxic table (David Kopf, Tujunga, CA), brain injection coordinates relative to Bregma were posterior 0.8 mm, lateral ± 0.5 mm, ventral 4.7 mm, corresponding to the paraventricular nucleus of the hypothalamus (15). 0.5 μl of virus (1×10^9 plaque-forming units/μl) was injected bilaterally over 10 min using a 26-gauge guide cannula and a 33-gauge injector (PlasticsOne, Roanoke, VA) connected to a Hamilton syringe and a syringe infusion pump (World Precision Instruments, Sarasota, FL). Injection with adeno-associated viral vector (rAAV) expressing Cre-recombinase produced hypothalamus-specific Y1 receptor knock-out mice ($Y1^{Hyp}$). Control $Y1^{lox/lox}$ mice were injected with virus carrying an empty adeno-associated viral vector and are referred to as $Y1^{lox/lox}$. Mice were housed individually for the ensuing 9 weeks, and body weight was measured three to five times per week at the same time of day.

Temperature Measurements—At 5 weeks after rAAV vector injection, body temperature was measured at ~9.00 h with a rectal thermometer (Physitemp Instruments Inc., Clifton, NJ). Temperature readings were taken within 10 s of removing the mouse from its cage. Repeat readings were taken from each mouse on 3 consecutive days, and the average of the three readings was used for statistical analysis.

Feeding and Behavioral Studies—At 6 weeks after rAAV vector injection, mice were transferred from housing on soft bedding to cages with only a single paper towel on the bottom of the cage and allowed to acclimatize for 3 nights. 24-h food and water intake were determined as the average of triplicate readings taken over 3 consecutive days. Actual food intake was calculated as the weight of pellets taken from the food hopper minus the weight of food spilled in the cage. Fecal weight was also determined in triplicate during these analyses. Wild-type mice housed on paper toweling typically used this to build a nest. This "nesting behavior" was quantified by weighing the amount of paper towel that had been shredded. 7 weeks post injection, the effect of 24 h fasting on body weight was determined. Food and water consumption, food spillage, and fecal output were determined as described above after 1 and 2 days of re-feeding, and body weight was also tracked during the first 3 days of re-feeding. Mice were then returned to soft bedding.

Glucose Tolerance Tests—At 8 weeks after rAAV vector injection, mice were fasted for 24 h before intraperitoneal injection of a 10% D-glucose solution (1.0 g/kg) with tail blood sampling (~20–50 μl) at 0, 15, 30, 60, and 120 min after injection. Serum was stored at −20 °C for subsequent analysis.

Tissue Collection—Mice were injected with the fluorescent compound calcein (15 mg/kg, Sigma) 10 and 3 days prior to tissue collection to enable subsequent calculation of bone formation rate. $Y1^{Hyp}$ mice and $Y1^{lox/lox}$ controls were culled at 18–19 weeks of age, 9 weeks after rAAV vector injection. Germ line $Y1^{-/-}$, $Y2^{-/-}$, and $Y1^{-/-}Y2^{-/-}$ mice and wild-type controls were culled at 15–17 weeks of age. Mice were culled in the freely fed state between 12:00 noon to 3:00 p.m. by cervical dislocation followed by decapitation for collection of trunk blood. Serum was collected and stored at −20 °C until subsequent analysis as described below. The interscapular brown adipose tissue (BAT) as well as white adipose tissue (WAT) depots (right inguinal, right epididymal or periovarian (gonadal), right retroperitoneal, and mesenteric) were removed and weighed. The weight of these WAT depots were summed together and expressed as total WAT weight, normalized as a percentage of body weight. Both femurs and the caudal vertebrae were excised and fixed in 4% paraformaldehyde for 16 h at 4 °C.

Bone Histomorphometry—The right femur was bisected transversely at the midpoint of the long axis, the distal half was embedded undecalcified in methacrylate resin (Medim-Medizinische Diagnostik, Giessen, Germany), and 5-μm sagittal sections were analyzed, as previously described (16). The 4th caudal vertebra was sectioned in the sagittal plane, and mid vertebral sections were analyzed as previously described (17). Briefly, sections were stained for mineralized bone, and trabecular bone volume, thickness, and trabecular numbers were calculated. Bone formation (mineralizing surface), mineral apposition rate, and bone formation rate were calculated, as previously described (16) using fluorescence microscopy (Leica, Heerbrugg, Switzerland). Osteoclast surface and osteoclast number were estimated using tartrate-resistant acid phosphatase-stained sections, with only multinucleated, tartrate-resistant acid phosphatase-positive cells associated with the bone surface being included in the analysis. Cortical mineral apposition rate was measured on the anterior periosteal surface in a region extending 1000 μm distal from the midpoint and in an endosteal region extending 1000 μm proximal from the posterior aspect of the growth plate, as previously described (18).

Bone Densitometry—Whole femoral bone mineral content and bone mineral density were measured using a dedicated mouse dual x-ray absorptiometer (Lunar Piximus II, GE Medical Systems, Madison, WI) in excised left hind limbs. Femurs were scanned with tibiae attached and the knee joint in flexion to 90°, to ensure consistent placement and scanning of the sagittal profile.

Quantitative Computed Tomography—Quantitative computed tomography was used to isolate cortical bone for analysis in male mice, using a Stratec XCT Research SA (Stratec Medizintechnik, Pforzheim, Germany). Scans were conducted using a voxel size of 70 μm, scan speed of 5 mm/s, and slice width of 0.2 mm every 0.5 mm on excised left femurs, as previously described (16). Bones were scanned in two consecutive slices, 7 and 7.5 mm from the distal margin of the femur, representing a mid femoral aspect. Bone strength index, an indicator of bending strength, was calculated (18).

Serum Analyses—Hormone levels in serum samples collected at cull were determined with commercial radioimmunoassay kits: insulin (Linco Research, St. Louis, MO), corticosterone, free T4 (ICN Biomedicals, Costa Mesa, CA), and insulin-like growth factor-1 (Bioclone Australia, Marrickville, New South Wales, Australia). Basal and glucose-induced serum glucose and insulin levels were determined with a glucose oxidase kit (Trace Scientific, Melbourne, Australia) and insulin with an enzyme-linked immunosorbent assay kit from Linco Research, respectively.

Gene Expression in Mouse Calvarial Osteoblast Cultures—Bone cells were isolated from calvariae of 2- to 3-day-old CsA mice using a modified time sequential enzyme-digestion technique (19). Cells from populations 6 to 10 were used. These cells showed an osteoblastic phenotype as assessed by their cAMP responsiveness to parathyroid hormone, expression of alkaline phosphatase, osteocalcin and bone sialoprotein, and the capacity to form mineralized bone noduli (data not shown). The cells were seeded in culture flasks containing α-minimal essential medium supplemented with 10% fetal calf serum, L-glutamine, and antibiotics at 37 °C in humidified air containing 5% CO_2.

After 4 days in flasks, the cells were seeded in culture dishes. Osteoblasts were plated at a density of 10^4 cells/cm^2 in culture dishes containing α-minimal essential medium/10% fetal bovine serum. After attachment overnight, medium was changed to α-minimal essential medium/10% fetal bovine serum. After 7 days of culture, RNA was extracted and used for quantitative real-time reverse transcription-PCR analyses.

RNA Extraction and cDNA Synthesis—Total RNA was extracted from mouse calvarial osteoblasts using the RNAqueous®-4PCR kit following the manufacturer's protocol (Ambion Inc., Austin, TX). The RNA was quantified spectrophotometrically, and the integrity of the RNA preparations was examined by agarose gel electrophoresis. Extracted total RNA was treated with deoxyribonuclease I to eliminate genomic DNA according to manufacturer instructions. One microgram of total RNA, following DNase treatment, was reverse transcribed into single-stranded cDNA with a 1st Strand cDNA Synthesis Kit using oligo-p(dT)15 primers. After incubation at 25 °C for 10 min and at 42 °C for 60 min, the avian myeloblastosis virus reverse transcriptase

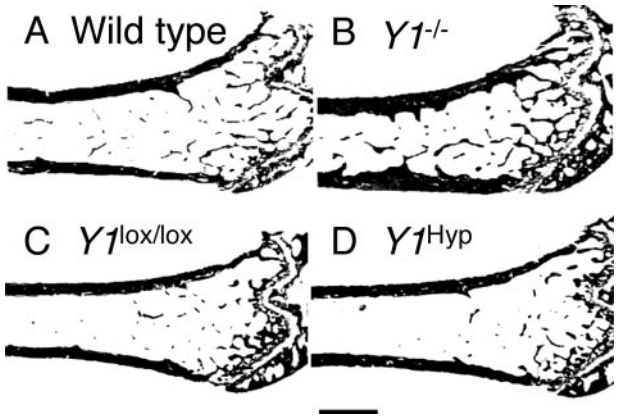

FIGURE 1. **Sagittal micrographs of the distal femoral metaphysis of (*B*) germ line $Y1^{-/-}$ male mice compared with (*A*) wild-type male controls or (*D*) male mice 9 weeks after hypothalamic injection of Cre-expressing rAAV vector to induce adult-onset hypothalamus-specific Y1 receptor deletion ($Y1^{Hyp}$) compared with (*C*) control mice injected with empty AAV vector ($Y1^{lox/lox}$).** Shown are darkly stained bone tissues representative of the respective groups. *Bar*, 1 mm.

was denatured at 99 °C for 5 min, followed by cooling to +4 °C for 5 min. The cDNA was kept at −20 °C until used for PCR.

Quantitative Real-time PCR—Expression of Y1 and Y2 receptor mRNA were analyzed by quantitative real-time PCR using the TaqMan Universal PCR master mix (Applied Biosystems, Foster City, CA) and a sequence detection system (ABI Prism 7900 HT Sequence Detection System and Software, Applied Biosystems) with fluorescence-labeled probes (reporter fluorescent dye VIC at the 5′-end and quencher fluorescent dye tetramethylrhodamine at the 3′-end). Primers and probes for Y1 and Y2 receptors were analyzed using a kit from Applied Biosystems. To control for variability in amplification due to differences in starting mRNA concentrations, β-actin was used as an internal standard. The specific primers and probes used are as follows for β-actin (sense: 5′-GGACCTGACGGACTACCTCATG-3′, antisense: 5′-TCTTTGATGTCACGCACGATTT-3′, probe: 5′-CCTGACCGAGCGTGGCTACAGCT TC-3′). The relative expression of target mRNA was computed from the target Ct values and the β-actin C_t value using the standard curve method (User Bulletin 2, Applied Biosystems).

Isolation and Culture of Bone Marrow Stromal Cells—Bone marrow stromal cells were isolated from 5- to 9-week-old male wild-type and germ line $Y1^{-/-}$ mice as previously described (see accompanying report (39)). Briefly, marrow was flushed from femurs and tibias with control media, and cells were plated at a density of 1.9×10^6 cells/cm^2 in 50-cm^2 plastic tissue culture plates. The non-adherent cell population was removed by medium changes 3 and 5 days later. Cells were trypsinized after 7 days in culture with 0.25% trypsin containing 0.53 mM EDTA and re-plated at 3×10^4 cells/cm^2 in 24-well plates in either control media or control media containing 100 nM human NPY (Auspep, Parkville, Victoria, Australia). After an additional 5 or 20 days in culture, cells were trypsinized, and viable cell numbers were determined by trypan blue staining.

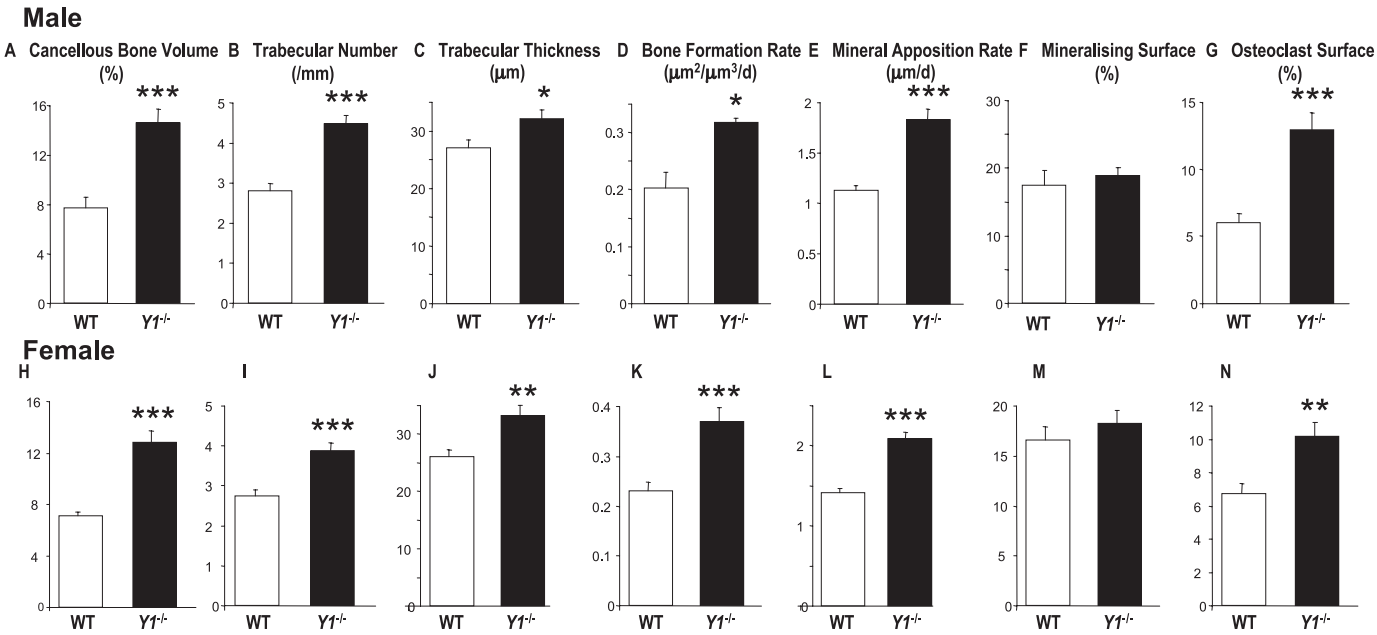

FIGURE 2. **Cancellous bone phenotype in the distal femoral metaphysis of male and female germ line *Y1*$^{-/-}$ mice.** Changes were consistent across both sexes, with lack of Y1 signaling resulting in greater cancellous bone volume (*A* and *H*), trabecular number (*B* and *I*), and trabecular thickness (*C* and *J*). These changes in bone were coincident with greater bone formation rate (*D* and *K*) due to greater mineral apposition rate (*E* and *L*) with no change in mineralizing surface (*F* and *M*). The cancellous bone surface covered by bone-resorbing cells was also altered, with osteoclast surface greater in *Y1*$^{-/-}$ compared with wild type (*G* and *N*). Data are means ± S.E. of 13–18 male mice and 10–13 female mice per group. *, $p < 0.05$; **, $p < 0.01$; and ***, $p < 0.001$ *versus* wild-type mice of the same gender.

Statistical Analyses—All data are expressed as mean ± S.E. Differences between two groups were assessed by two-tailed Student's *t* test. Differences among multiple groups of mice were assessed by analysis of variance or repeated measures analysis of variance, followed by Fisher's or Contrast post-hoc comparisons if appropriate (StatView version 4.51 or SuperANOVA, Abacus Concepts Inc., Berkeley, CA). Statistical significance was defined as $p < 0.05$.

RESULTS

Greater Bone Formation in Y1 Receptor Null Mice

To examine the mechanism behind the elevation in bone mass evident in Y1$^{-/-}$ mice (see accompanying report (39)), we examined distal femurs and caudal vertebrae from skeletally mature male and female mice.

Cancellous Bone—Germ line *Y1*$^{-/-}$ mice displayed significantly greater cancellous bone volume in the distal femoral metaphysis, with greater trabecular number and thickness (Figs. 1 and 2). Interestingly, this was associated with increased activity of both osteoblastic and osteoclastic lineages. Similar to *Y2*$^{-/-}$ mice, bone formation rate was greater in *Y1*$^{-/-}$ mice compared with wild-type mice with enhanced mineral apposition rate (MAR) in both sexes, but no change in mineralizing surface (Fig. 2). However, in contrast to *Y2*$^{-/-}$ mice, bone resorption was also altered in *Y1*$^{-/-}$ mice, with significantly greater osteoclast surface in both sexes (Fig. 2).

These changes in cancellous bone homeostasis were also evident in the caudal vertebrae. At this site, cancellous bone volume was significantly increased in knock-out mice compared with wild-type values (*Y1*$^{-/-}$, 30.9 ± 1.2% *versus* wild type, 25.5 ± 2.4%, $n = 5$–9 male mice, $p < 0.05$). As in the femurs, this change was also associated with greater trabecular thickness (*Y1*$^{-/-}$, 65.4 ± 2.0 μm *versus* wild type, 44.0 ± 2.9 μm, $p < 0.0001$). These cancellous changes are consistent with the previously noted elevation in bone mineral density and content in *Y1*$^{-/-}$ long bones; however, because cortical bone rather than

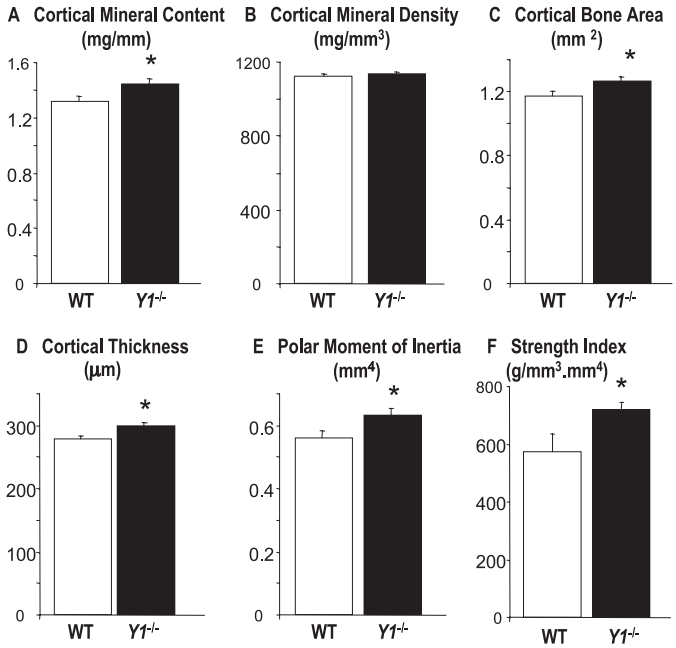

FIGURE 3. **Cortical bone phenotype in the mid-femoral diaphysis of male germ line *Y1*$^{-/-}$ mice.** Cortical mineral content (*A*) was greater in *Y1*$^{-/-}$ mice compared with wild-type mice, with no change in cortical mineral density (*B*). This was coincident with greater cortical bone area (*C*) and thickness (*D*). Strength indices were also altered, with polar moment of inertia (*E*) and calculated strength index (*F*) greater in *Y1*$^{-/-}$ compared with wild-type mice. Data are means ± S.E. of six to eight male mice per group. *, $p < 0.05$ *versus* wild type.

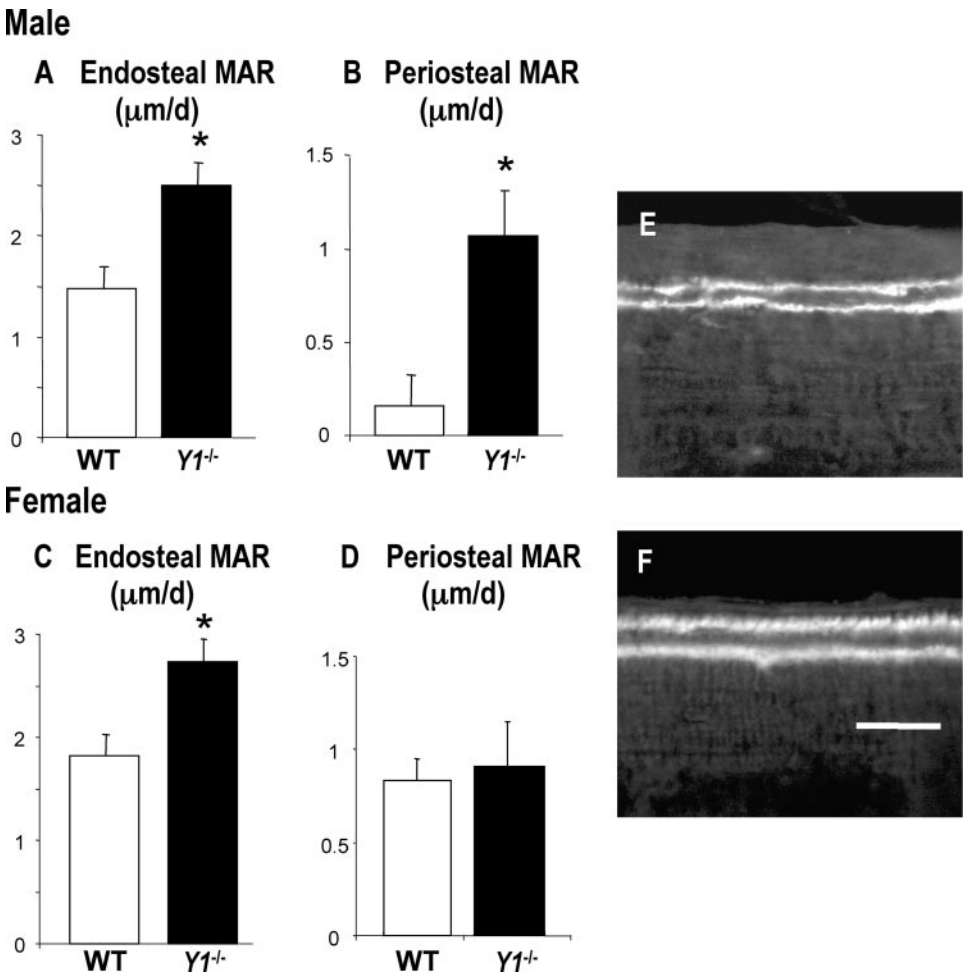

FIGURE 4. **Cortical bone formation in femurs of germ line *Y1*$^{-/-}$ mice.** Endosteal mineral apposition rate (MAR) was greater in both sexes of *Y1*$^{-/-}$ mice (*A* and *C*), with periosteal MAR greater in males only (*B* and *D*). Data are means ± S.E. of five to seven male and seven or eight female mice per group. Photomicrographs show calcein label apposition on the periosteal surface of male wild-type (*E*) and *Y1*$^{-/-}$ (*F*) mice, with an interlabel interval of 7 days. *Bar*, 12 μm. *, $p < 0.05$ *versus* wild-type mice of the same gender.

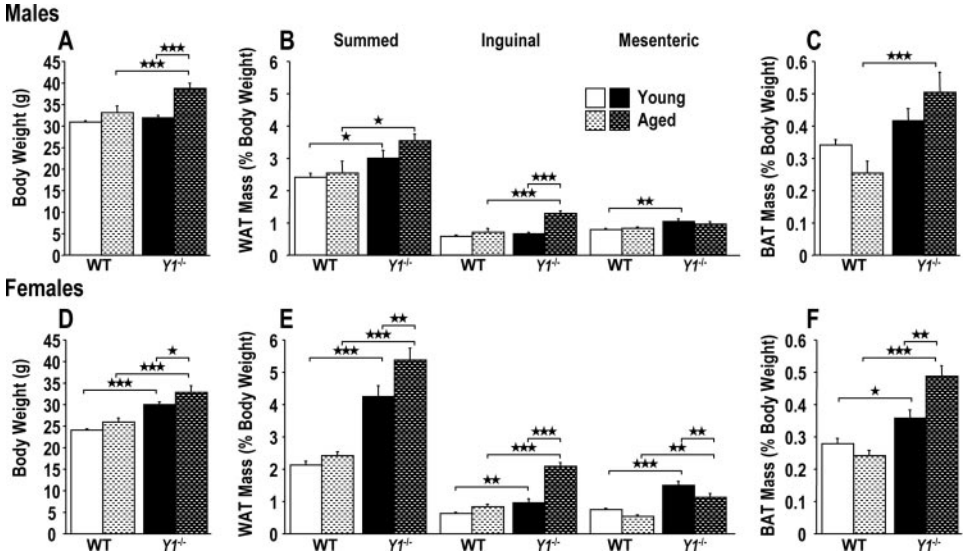

FIGURE 5. **Changes in body weight (*A* and *D*) and adiposity (*B*, *C*, *E*, and *F*) of young (15–17 weeks) and aged (46–52 weeks) male and female germ line *Y1*$^{-/-}$ mice.** The mass of WAT depots (right inguinal, right epididymal or right periovarian, right retroperitoneal, and mesenteric), expressed as a percentage of body weight, were summed (*B* and *E*). *C* and *F*, BAT. Data are means ± S.E. of at least 15 young and at least 7 aged mice per group. *, $p < 0.05$; **, $p < 0.01$; and ***, $p < 0.001$ *versus* the comparison shown by *horizontal bars*.

cancellous bone is the major contributor to changes in bone density and content, the cortical content of bones from Y1$^{-/-}$ mice was further examined.

Cortical Bone—Cortical changes in *Y1*$^{-/-}$ long bones were examined by quantitative computed tomography. At the mid-femur, *Y1*$^{-/-}$ mice had greater cortical mineral content and density, consistent with greater cortical area and thickness (Fig. 3). Polar moment of inertia and strength index were also significantly greater in the femoral cross-sections of *Y1*$^{-/-}$ compared with wild-type mice (Fig. 3). The observed increase in cortical mineral content in *Y1*$^{-/-}$ mice combined with the 25% increase in strength index indicate a response sufficient to produce functional relevant changes in bone strength *in vivo* and highlights the therapeutic potential of such pathways.

To further investigate the cellular basis for these differences, both endocortical and periosteal surfaces were examined. Cortical osteoblast activity was increased in *Y1*$^{-/-}$ mice, with MAR elevated on the femoral endosteal surface an average of 70% in both genders and on the periosteum of male *Y1*$^{-/-}$ mice with an increase of nearly 7-fold (Fig. 4). Taken together, these data reveal that loss of Y1 receptor signaling results in a generalized elevation in parameters of osteoblast activity, at both axial and appendicular sites leading to greater cancellous and cortical bone accrual.

Sustained Elevation of Adiposity in Y1 Receptor Null Mice—Body weight and adiposity of young and aged *Y1*$^{-/-}$ mice were compared with age-matched wild-type controls to determine progression of the *Y1*$^{-/-}$ energy homeostasis phenotype. Both male and female *Y1*$^{-/-}$ mice developed an obese phenotype with advancing age (Fig. 5), indicated by significantly greater body weight, WAT and BAT depots, and with a more pronounced phenotype in female *Y1*$^{-/-}$ mice. These changes in body weight were not due to changes in stature, because femur

length was not significantly different between $Y1^{-/-}$ mice and wild type (data not shown). Thus, whereas wild-type mice showed no changes in body weight and adiposity with age beyond 12 months, $Y1^{-/-}$ mice showed marked and significant increases, indicating a sustained and continuing effect on energy homeostasis and adipocyte function in these mice.

To gain insight into possible mechanisms of obesity associated with Y1 deficiency, we measured metabolic parameters and energy expenditure in $Y1^{-/-}$ mice. There was no significant effect of genotype on serum concentrations of corticosterone, glucose, insulin-like growth factor 1, and free T4 and temperature (data not shown); however, serum insulin levels were significantly higher in $Y1^{-/-}$ mice (female $Y1^{-/-}$, 177 ± 27 pM *versus* wild type, 56 ± 7 pM, $n = 17$, $p < 0.001$; male $Y1^{-/-}$, 220 ± 52 pM *versus* wild type, 120 ± 18 pM, $n = 18$, $p < 0.05$). Because insulin is lipogenic (20–22), it is possible that these higher serum insulin levels may be causally linked to the greater adiposity observed in young and aged germ line $Y1^{-/-}$ mice.

Interestingly, and in contrast to the elevated adiposity, $Y1^{-/-}$ mice displayed significant reductions in food intake at 1, 2, and 8 h after re-introduction of food following 24-h fasting (*e.g.* female $Y1^{-/-}$, 0.95 ± 0.12 g/2 h *versus* wild type, 2.12 ± 0.36 g/2 h, $n = 4$, $p < 0.01$; male $Y1^{-/-}$, 1.33 ± 0.16 g/2 h *versus* wild type, 2.30 ± 0.33 g/2 h, $n = 4$, $p < 0.01$), whereas no such reduction in food intake was apparent in $Y1^{-/-}$ mice in the non-fasted state or beyond 24 h of re-feeding.

TABLE 1

Cancellous bone parameters in the femur following adult-onset hypothamus-specific deletion of Y1 receptors ($Y1^{Hyp}$) compared to control mice with Y1 receptors intact ($Y1^{lox/lox}$)

Data are means ± S.E. of three to five male and seven to ten female mice per group. At $p < 0.05$, no significant differences were detected in within-gender comparisons.

Genotype/ gender	Cancellous bone volume	Mineral apposition rate	Osteoclast surface	Osteoclast number
	%	μm/d	%	/mm
Male				
$Y1^{lox/lox}$	8.0 ± 0.7	2.24 ± 0.1	13.0 ± 0.5	4.5 ± 0.3
$Y1^{Hyp}$	7.0 ± 2.0	1.98 ± 0.2	14.3 ± 2.2	5.2 ± 0.8
Female				
$Y1^{lox/lox}$	7.2 ± 0.8	2.63 ± 0.1	12.1 ± 1.1	3.9 ± 0.3
$Y1^{Hyp}$	9.4 ± 0.9	2.48 ± 0.1	12.5 ± 1.2	3.9 ± 0.4

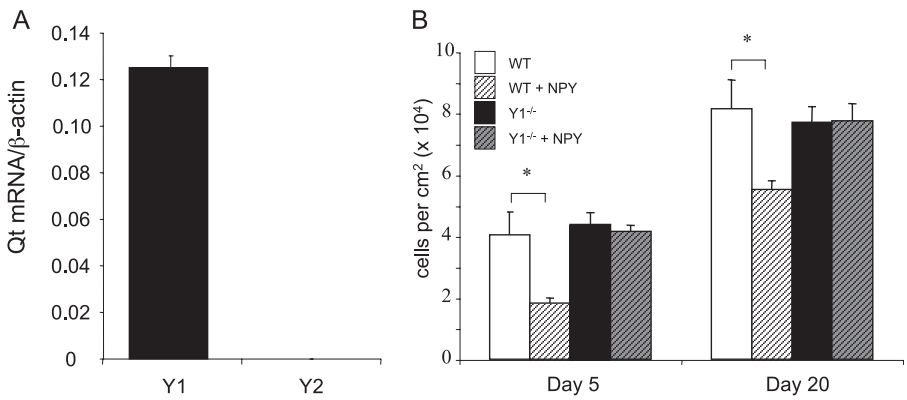

FIGURE 6. **Expression of Y1 and Y2 receptor mRNA.** Graph showing quantitative real-time reverse transcription-PCR analysis of Y1 receptor expression in mouse calvarial osteoblasts (*A*). The values shown are quantity (*Qt*) of Y1 receptor mRNA normalized to that of β-actin. Data are mean $n = 5$ ± S.E. *B*, effect of NPY treatment on the number of viable bone marrow stromal cells from wild-type and $Y1^{-/-}$ mice. Treatment of cultures with 100 nM NPY significantly decreased cell number in the wild-type cultures but not in cultures derived from $Y1^{-/-}$ mice. $p < 0.01$ *versus* the comparison shown.

Hypothalamic Y1 Receptors Do Not Regulate Bone Mass—Previously we showed that hypothalamus-specific Y2 receptor deletion leads to pronounced anabolic effects on bone (1). We therefore hypothesized that the phenotype observed in the bones of germ line $Y1^{-/-}$ mice might also involve signals mediated by the hypothalamus. To test this, we investigated bone homeostasis in mice with adult-onset, hypothalamus-specific deletion of Y1 receptors. Localized Y1 receptor deletion in the hypothalamus was verified by PCR on genomic DNA extracted from the hypothalamus, with forebrain and liver of rAAV vector-injected mice used as negative controls. PCR primers were designed to produce a detectable product only when the Y1 receptor had been deleted. This was the case only in amplified DNA extracted from the hypothalamus of virus-injected $Y1^{lox/lox}$ mice but not in DNA from control samples (data not shown), confirming the successful ablation of Y1 receptor genes in this area.

Cancellous Bone—Deletion of hypothalamic Y1 receptors from adult mice ($Y1^{Hyp}$) did not alter cancellous bone volume compared with age-matched $Y1^{lox/lox}$ controls of either sex (Fig. 1 and Table 1). Importantly, and consistent with the lack of change in cancellous bone volume, hypothalamus-specific deletion of Y1 receptors did not alter bone cell activity. Mineral apposition rate and osteoclast surface and number were not different between $Y1^{Hyp}$ and $Y1^{lox/lox}$ controls of either gender (Table 1).

Cortical Bone—Similarly, quantitative computed tomography analysis revealed no difference in cortical bone between $Y1^{Hyp}$ and $Y1^{lox/lox}$ groups, with no change in femoral BMC in males ($Y1^{Hyp}$, 1.28 ± 0.03 g *versus* $Y1^{lox/lox}$, 1.29 ± 0.03 g, $n = 3$–5) or females ($Y1^{Hyp}$, 1.17 ± 0.02 g *versus* $Y1^{lox/lox}$, 1.15 ± 0.04 g, $n = 3$–5). Femoral bone marrow density was not different in males ($Y1^{Hyp}$, 758 ± 13 mg/mm^2 *versus* $Y1^{lox/lox}$, 754 ± 10 mg/mm^2, $n = 3$–5) or females ($Y1^{Hyp}$, 766 ± 7 *versus* $Y1^{lox/lox}$, 747 ± 6 mg/mm^2, $n = 3$–5). No change in cortical mineral content, density, or architecture was observed (data not shown). These findings demonstrate that Y1 receptors in this part of the brain are not responsible for the marked effects of germ line Y1 receptor knock-out on bone and further indicate a peripheral, possibly direct, site of action.

Y1 Receptor Mediates Direct Effects of NPY on Bone Marrow Stromal Cell Number—To investigate the possibility that Y1 receptors influence bone tissue via direct effects, Y1 receptor expression was investigated in mouse calvarial osteoblasts expressing the osteoblastic marker genes alkaline phosphatase, osteocalcin, and bone sialoprotein, and demonstrating the capability of forming mineralized bone noduli (data not shown). Quantitative real-time PCR revealed that Y1 receptor gene transcripts were present in osteoblasts at day 7 of culture (Fig. 6*A*). Expression of Y2 receptors was

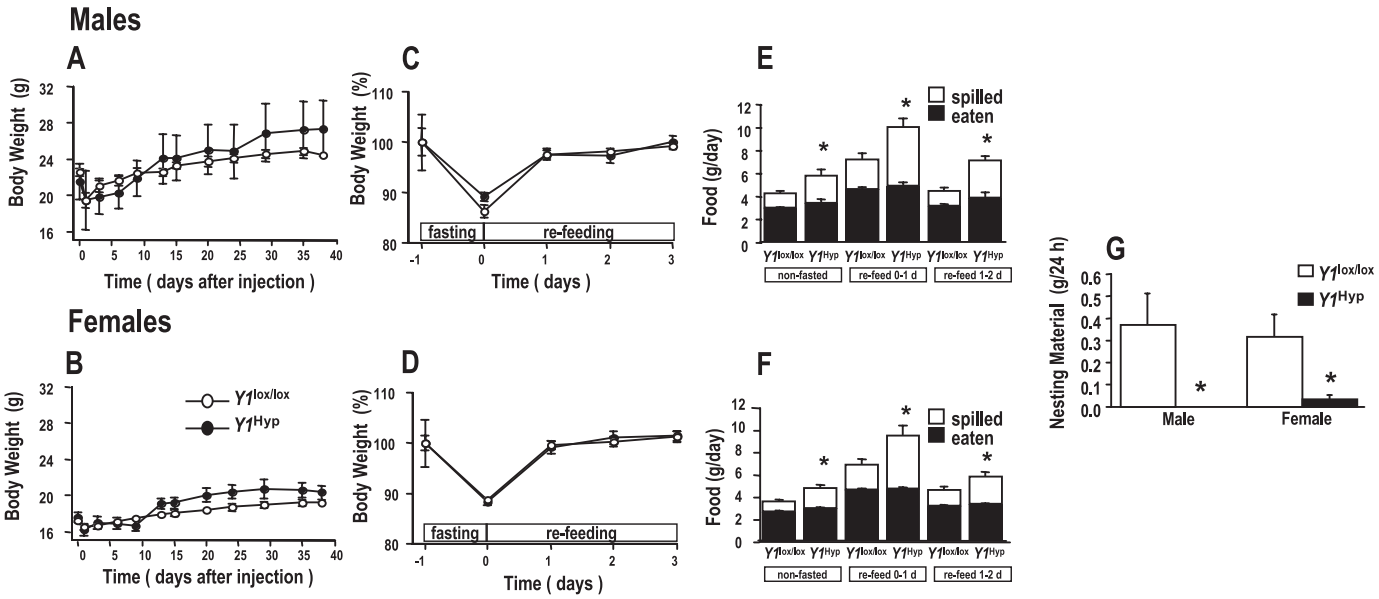

FIGURE 7. **Effect of hypothalamus-specific Y1 receptor deletion on non-fasted and fasting-induced body weight, feeding, and nesting behavior.** Region-specific Y1 receptor knock-out, in the hypothalamus ($Y1^{Hyp}$) on day 0, had no significant effect on body weight (*A* and *B*) compared with control mice ($Y1^{lox/lox}$). Shown are the percent body weight values lost during 24-h fasting and 72-h re-feeding (*C* and *D*) and feeding behavior incorporating the amount of food taken from the food hopper but spilled on the cage floor as well as the amount of food actually eaten, either in the non-fasted state (before fasting) or in the first 48 h of re-feeding (*E* and *F*). *G*, nesting behavior, quantified as the weight of paper toweling shredded per day. Data in *panels C–G* were collected at 7 weeks after adenoviral vector injection. Data are means ± S.E. of four or five male and seven to ten female mice per group. *, $p < 0.05$ *versus* the amount of food spilled or the amount of paper toweling shredded by control ($Y1^{lox/lox}$) mice of the same gender and of the same nutritional status (non-fasted or re-fed).

TABLE 2

Effect of hypothalamus-specific deletion of Y1 receptors on parameters of energy balance in adult mice

Data are means ± S.E. of three to five male and seven to ten female mice. At $p < 0.05$, no significant differences were detected in within-gender comparisons.

Genotype	Body weight	Water intake	Fecal output	WAT weight	BAT weight	Rectal temperature	Fasting serum glucose	Area under glucose tolerance curve (glucose)	Fasting serum insulin	Area under glucose tolerance curve (insulin)
	g	*ml/day*	*g/day*	*% BWT*[a]	*% BWT*	*°C*	*mM*	*mMx90*	*pM*	*pMx90*
Male										
$Y1^{lox/lox}$	27.2 ± 1.3	3.5 ± 0.2	0.83 ± 0.05	2.8 ± 0.3	0.29 ± 0.02	35.74 ± 0.3	5.0 ± 1.1	670 ± 90	62 ± 2	8,520 ± 440
$Y1^{Hyp}$	27.0 ± 3.8	4.2 ± 0.8	0.76 ± 0.08	3.9 ± 1.4	0.44 ± 0.16	35.73 ± 0.3	6.5 ± 0.8	750 ± 200	80 ± 17	10,640 ± 40
Female										
$Y1^{lox/lox}$	19.6 ± 0.4	4.0 ± 0.4	0.64 ± 0.03	3.0 ± 0.2	0.33 ± 0.03	36.11 ± 0.2	5.3 ± 0.4	730 ± 50	89 ± 6	11,180 ± 570
$Y1^{Hyp}$	20.9 ± 0.9	4.7 ± 0.3	0.60 ± 0.04	3.0 ± 0.5	0.27 ± 0.02	36.51 ± 0.2	5.0 ± 0.6	810 ± 80	97 ± 13	13,040 ± 710

[a] %BWT, percent body weight.

not detected. These data are consistent with a direct, Y1-mediated effect in these cells. To further investigate this possibility, the effect of NPY treatment on cultured bone marrow stromal cells from wild-type and $Y1^{-/-}$ mice was examined. Administration of NPY to cultures from wild-type tissue markedly reduced cell numbers (Fig. 6*B*). Cell numbers in $Y1^{-/-}$ cultures were comparable to those of wild-type control cultures and were not altered by NPY treatment, providing the first evidence of direct, Y1-mediated regulation of this system.

Hypothalamic Y1 Receptors Do Not Alter Energy Homeostasis—Hypothalamic Y1 receptors are hypothesized to mediate anabolic effects, namely hyperphagia, under conditions of elevated hypothalamic NPY levels such as fasting or genetic obesity (10, 11). We investigated energy homeostasis in $Y1^{Hyp}$ mice but did not see significant differences from control $Y1^{lox/lox}$ mice with respect to body weight in the first 6 weeks after rAAV vector injection, at time of cull 9 weeks after vector injection, or in response to 24-h fasting and 72-h re-feeding (Fig. 7 and Table 2). The actual food intake of $Y1^{Hyp}$ mice was not significantly different from that of control mice (Fig. 7), either in the non-fasted state or in the first 2 days of re-feeding after a 24-h fast. In keeping with a lack of effect of hypothalamic Y1 receptor deletion on food intake, water intake and fecal output were not significantly different between $Y1^{Hyp}$ and $Y1^{lox/lox}$ mice (Table 2).

Some factors that regulate energy homeostasis do so by altering fat mass or glucose metabolism even in the absence of effects on body weight or food intake (10, 21, 23, 24). We therefore investigated whether hypothalamic Y1 receptor knock-out induced alterations in fat mass or glucose homeostasis. $Y1^{Hyp}$ mice showed no significant difference from $Y1^{lox/lox}$ mice with respect to WAT and BAT depots or rectal temperature (Table 2), suggesting no change in thermogenesis. In addition, there was no significant effect on fasting serum glucose or insulin levels or the change in serum glucose or insulin levels in response to intraperitoneal glucose injection, albeit the area under the insulin curve after glucose injection tended to be higher in knock-out than in wild-type mice (Table 2).

The conditional deletion of Y1 receptors in adult mice has, for the first time, enabled examination of the role of these signals in

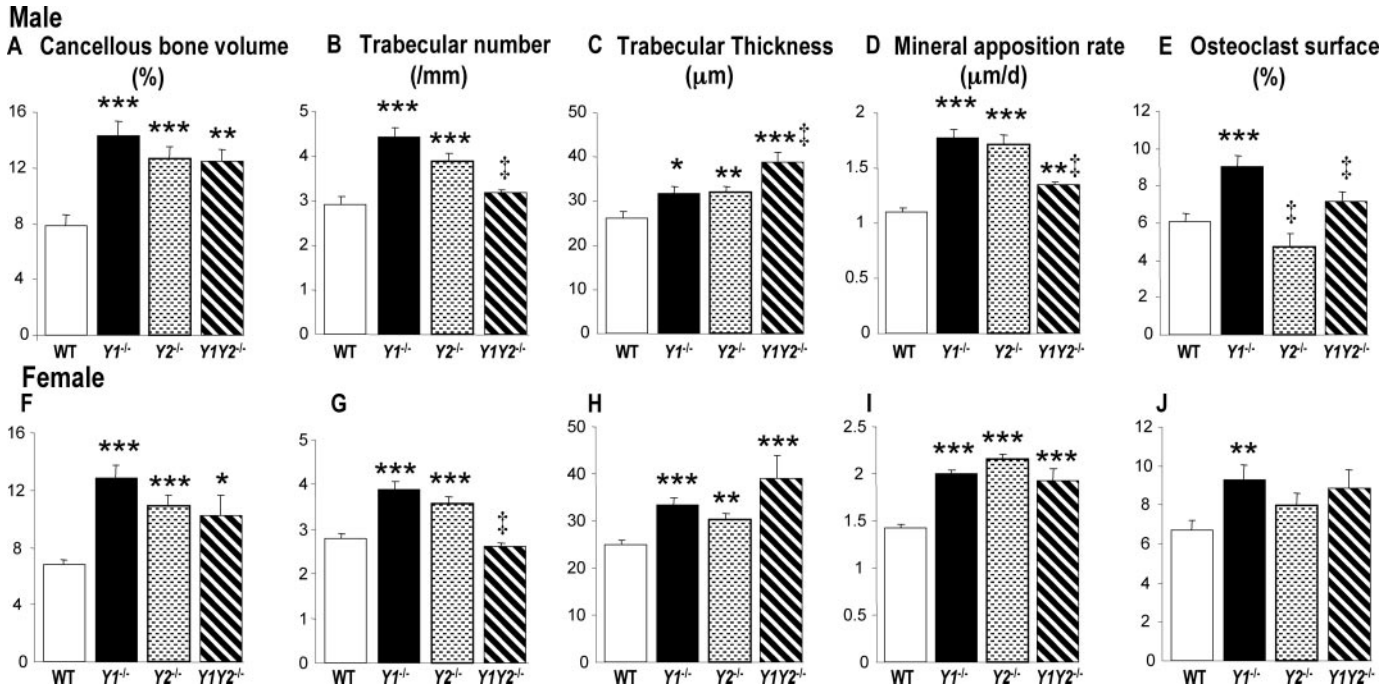

FIGURE 8. **Cancellous bone phenotype in the distal femoral metaphysis of male and female germ line Y1, Y2, and $Y1^{-/-}Y2^{-/-}$ receptor double knock-out mice.** Changes were consistent across both sexes, with lack of Y1 receptor signaling resulting in greater cancellous bone volume (*A* and *F*) and trabecular thickness (*C* and *H*) with trabecular number (*B* and *G*) greater in $Y1^{-/-}$ and $Y2^{-/-}$ mice only. These changes were coincident with greater mineral apposition rate (*D* and *I*). Parameters of bone resorption were also altered, with osteoclast surface (*E* and *J*) greater in $Y1^{-/-}$ mice compared with wild-type controls. Data are means ± S.E. of 13–18 male and 10–13 female mice per group. *, $p < 0.05$; **, $p < 0.01$; and ***, $p < 0.001$ *versus* wild-type mice of the same gender; ‡, $p < 0.05$ *versus* $Y1^{-/-}$ mice of the same gender.

energy homeostasis. In a similar manner to skeletal effects, the regulation of energy homeostasis and food intake by Y1 is not controlled by those hypothalamic receptors that were deleted in the current study, indicating a consistent pattern of non-hypothalamic Y1 action in the regulation of these processes.

However, hypothalamic Y1 receptor knock-out did alter specific aspects of behavior in relation to feeding. Food grinding was markedly increased in these mice, with the amount of ground food spilled on the cage floor significantly elevated in both male and female $Y1^{Hyp}$ mice compared with controls (Fig. 7).

Hypothalamic Y1 Receptors Modify Behavior—Interestingly, although hypothalamus-specific Y1 receptor deletion had no impact on parameters of energy homeostasis, it significantly influenced a related maternal behavior, showing a loss of nest-building abilities. Whereas control $Y1^{lox/lox}$ mice consistently used the paper towel provided as bedding material for constructing a nest, this behavior was completely absent in $Y1^{Hyp}$ mice. Indeed, the measured weight of shredded paper, as an indicator for nesting behavior, was dramatically reduced in both male and female $Y1^{Hyp}$ *versus* $Y1^{lox/lox}$ control mice (Fig. 7).

Coincident Deletion of Y1 and Y2 Receptors Does Not Induce Additive Changes in Bone

Cancellous Bone—Our previous study revealed a Y2-dependent inhibition of Y1 expression in osteoblastic and adipocytic lineage cells (see accompanying report (39)), thereby suggesting a putative mechanism whereby central Y2 signaling modulates peripheral tissue homeostasis. To gain further insights into whether Y1 and Y2 receptors are linked in the regulation of bone physiology, we generated $Y1^{-/-}Y2^{-/-}$ receptor double knock-out mice and investigated whether additive effects were apparent. Importantly, although $Y1^{-/-}Y2^{-/-}$ receptor double knock-out mice of both genders had significantly greater cancellous bone volume compared with wild-type controls (Fig. 8), there were no significant differences from $Y1^{-/-}$ and $Y2^{-/-}$ mice. Mineral apposition rate was significantly increased in all three Y receptor-deficient models compared with wild-type mice. There were however, some minor differences, with MAR in male $Y1^{-/-}Y2^{-/-}$ mice significantly reduced compared with $Y2^{-/-}$ mice. Unlike $Y1^{-/-}$ mice, $Y1^{-/-}Y2^{-/-}$ mice showed no increase in osteoclast surface (Fig. 8). Thus, whereas double deletion of Y1 and Y2 receptors induces significant effects on cancellous bone, there were no obvious additive effects over those of Y1 or Y2 receptor deletion in isolation.

Cortical Bone—Similarly, quantitative computed tomography analysis revealed that $Y1^{-/-}Y2^{-/-}$ femurs had significantly greater cortical bone area and thickness than wild-type mice, although there was no significant effect on cortical mineral content or density (Fig. 9). As in the $Y1^{-/-}$ and $Y2^{-/-}$ single knock-out models, these architectural changes were coincident with greater cortical bone formation in $Y1^{-/-}Y2^{-/-}$ mice, with endosteal MAR elevated compared with wild type (Fig. 9). The strength index of femurs from $Y1^{-/-}Y2^{-/-}$ double knock-out mice was comparable to those in single $Y1^{-/-}$ or $Y2^{-/-}$ animals (Fig. 9). Although a common feedback control for independent pathways cannot be ruled out, the lack of additive responses in

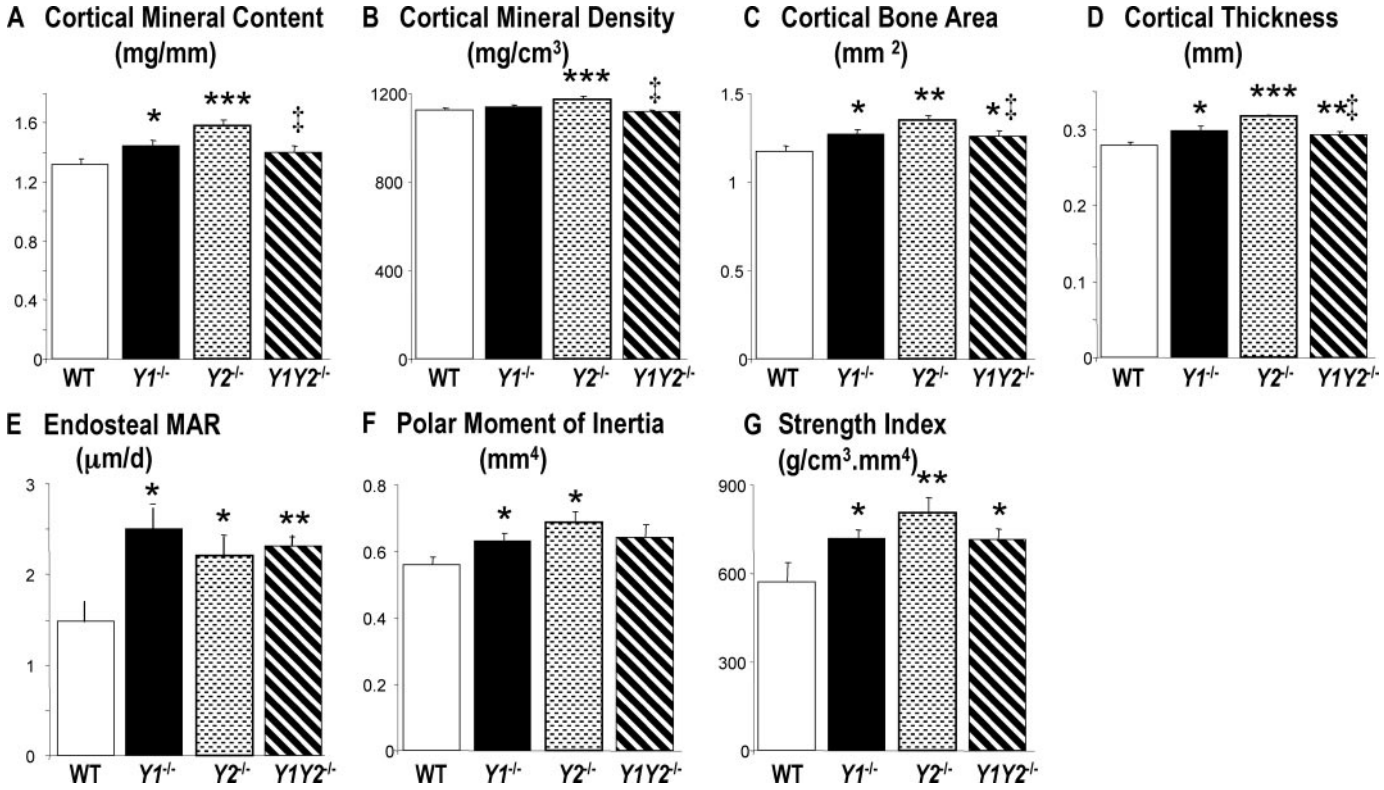

FIGURE 9. **Cortical bone phenotype in the mid-femoral diaphysis of male germ line Y1, Y2, and $Y1^{-/-}Y2^{-/-}$ receptor double knock-out mice.** Cortical mineral content (*A*) was greater in $Y1^{-/-}$ and $Y2^{-/-}$ mice compared with wild type. Compared with wild-type mice, cortical mineral density (*B*) was greater in $Y2^{-/-}$ mice only. Cortical bone area (*C*) and cortical thickness (*D*) were greater in all Y receptor-deficient mice, coincident with greater cortical bone formation, with endosteal mineral apposition rate (MAR, *E*) greater in all Y receptor-deficient mice. Strength indices were altered, with polar moment of inertia (*F*) greater in $Y1^{-/-}$ and $Y2^{-/-}$ mice and calculated strength index (*G*) greater in all Y receptor-deficient mice compared with wild-type controls. Data are means ± S.E. of six to eight mice per group. *, $p < 0.05$; **, $p < 0.01$; and ***, $p < 0.001$ *versus* wild-type mice; ‡, $p < 0.05$ *versus* $Y2^{-/-}$ mice.

$Y1^{-/-}Y2^{-/-}$ mice is consistent with a common pathway from the hypothalamus to bone involving both Y2 and Y1 signaling.

DISCUSSION

In this study we show that Y1 receptors exert powerful control over bone production and have significant effects on adiposity. These findings indicate that these effects are most likely mediated by non-hypothalamic Y1 receptors. Germ line disruption of Y1 receptor signaling revealed a generalized increase in osteoblast activity on both cancellous and cortical surfaces, with consistent changes in femoral, tibial, and vertebral bones. Expression of Y1 receptors on osteoblastic and bone marrow stromal cells suggested a peripheral, possibly direct mechanism of action. In keeping with this, deletion of hypothalamic Y1 receptors did not alter bone homeostasis and direct action of Y1 signaling was confirmed *ex vivo* in bone marrow stromal cell cultures, where the NPY-mediated inhibition of cell number was absent in $Y1^{-/-}$ cells. These findings are consistent with our previous study, with reduced expression of Y1 receptors in stromal cells associated with a greater number of mesenchymal progenitor cells in $Y2^{-/-}$ mice (see accompanying report (39)). Moreover, a common pathway controlling bone formation by Y1 and Y2 receptor subtypes was suggested by a lack of additive effects on bone in $Y1^{-/-}Y2^{-/-}$ mice.

In addition, adiposity was significantly elevated in young and aged $Y1^{-/-}$ mice, in association with significant decreases in fasting-induced hyperphagia and increases in serum insulin levels. Because insulin is lipogenic, promoting partitioning of fuels toward WAT and away from muscle (20, 22), the hyperinsulinemia observed in germ line Y1 knock-out mice could contribute to the increased adiposity observed in these animals despite the lack of hyperphagia. As with effects on bone, these changes in food intake and adiposity were not evident in mice following adult-onset deletion of hypothalamic Y1 receptors, indicating mediation of these effects by Y1 receptors other than those hypothalamic receptors that were deleted in the current study. Although hypothalamic Y1 receptors are not likely involved in regulation of bone or adipose tissue nor of non-fasted or fasting-induced food intake or body weight, they profoundly influenced feeding and nesting behaviors, with hypothalamus-specific Y1 receptor knock-out mice showing marked increases in food grinding behavior and a pronounced lack of nest-building behavior. Overall, these findings indicate a generalized and powerful peripheral action of Y1 signaling in the regulation of bone and adipose tissue.

Current understanding of the role of the NPY system in the regulation of bone tissue and energy balance is rapidly expanding. Y2 receptors have been established as significant regulators of both bone and adipose tissue, with Y2 receptor knock-out enhancing bone formation and reducing adiposity (1, 2, 25, 26). Coincident deletion of Y2 and Y4 receptors enhanced effects on bone and adipose tissue, with $Y2^{-/-}Y4^{-/-}$ knock-out mice showing even more pronounced increases in bone mass and

synergistic decreases in adiposity (3). We now demonstrate that loss of Y1 receptor signaling also altered bone tissue and energy homeostasis; however, the changes show important differences from $Y2^{-/-}$ or $Y2Y4^{-/-}$ mice, revealing unique actions of individual Y receptors. Loss of Y1 signaling led to an increase in adipose deposition, the opposite to that evident in lean $Y2^{-/-}$ and $Y2Y4^{-/-}$ mice. The regulation of fat and bone are to a certain extent related by the actions of leptin, acting in the hypothalamus to decrease adiposity and cancellous bone formation (27–29). This relationship is evident in $Y2Y4^{-/-}$ mice, whose lean phenotype and consequently reduced serum leptin is a likely mechanism for the increased bone volume compared with $Y2^{-/-}$ mice (3). Similarly, the obesity evident in $Y1^{-/-}$ mice might be expected to affect bone volume through action of increased circulating leptin concentrations. However, as previously shown, despite greater fat mass, serum leptin levels are not increased in our $Y1^{-/-}$ mice and indeed are not altered in $Y2^{-/-}$ or $Y1^{-/-}Y2^{-/-}$ mice (13), suggesting that the leptin and NPY-mediated pathways act separately in this model, as in previous studies (3, 16, 25).

Given the central nature of Y2-mediated effects on energy homeostasis (2), the Y1-deficient phenotype was also assessed by conditional deletion of hypothalamic Y1 receptors. The paraventricular nucleus was chosen due to its strategic location in the energy homeostasis circuit and because of the presence of Y1 receptor expression in this area as well as known NPY projections to this region from the arcuate nucleus (6). Interestingly, the effects on adipose tissue evident in germ line $Y1^{-/-}$ mice were absent in hypothalamus-specific Y1 receptor knock-out mice, demonstrating that the regulation of energy homeostasis is not directly mediated through those hypothalamic Y1 receptors deleted in this study but rather via other sites. Additionally, Y1 receptors are expressed in peripheral tissues, including pancreatic β cells (8), and are likely to mediate direct effects such as inhibition of insulin secretion (23, 30). Thus the hyperinsulinemia of $Y1^{-/-}$ mice may be a direct response to lack of Y1 receptors in pancreatic islet tissue and, given that insulin is lipogenic (20, 22), may contribute to the greater adiposity of these mice (13). Consistent with this action, the greatest change in adiposity was evident in $Y1^{-/-}$ females, which also had the greatest increase in serum insulin.

Although there is a lack of involvement of hypothalamic Y1 receptors in the regulation of energy homeostasis, these receptors play a significant role in the regulation of feeding and other feeding-related behavior. The exact reasons for food grinding in mice are not clear (31), although it has been shown that electrical and chemical stimulation of the hypothalamus influences the activity of masticatory trigmental neurons in the brain stem important for jaw movement (32). It is therefore possible that ablation of Y1 receptors in the hypothalamus leads to altered responses to these neurons in the brainstem, leading to increased grinding of food. Interestingly, electrical lesioning of the paraventricular nucleus has also been found to disrupt the initiation of maternal behavior, *e.g.* nest building in the rat (33). Considering the high level of Y1 receptors in the paraventricular nucleus, lack of Y1 receptors in this area might cause a similar alteration in mice and could explain at least part of the altered nest-building behavior seen in these conditional knockout mice.

Consistent with the adipose phenotype, and in contrast to the centrally mediated effects on bone in $Y2^{-/-}$ mice, the Y1-dependent changes in bone did not involve those receptors expressed in the hypothalamus (1). The importance of this peripheral action of Y1 is heightened by the presence of Y1 receptors in osteoblastic cells, indicating, as in adipose tissue and pancreatic β cells, the potential for direct effects. Moreover, the lack of NPY-mediated inhibition in $Y1^{-/-}$ bone marrow stromal cell cultures shows, for the first time, direct regulation of osteoblastic cells by NPY-mediated stimulation of Y1 receptors and is consistent with previous NPY effects in bone cells (34, 35). The putative regulatory role of these osteoblastic Y1 receptors is consistent with a growing understanding of the direct effects of neural signaling molecules on bone cell activity. Adrenergic (36), glutamatergic (37), and cannabinoid (38) receptors are among those neural signals recently described as directly mediating changes in bone homeostasis. Although similar to $Y2^{-/-}$ mice with respect to osteoblastic effects, the bone phenotype of $Y1^{-/-}$ mice was different from that of $Y2^{-/-}$ mice, in that Y1 receptor knockouts displayed involvement of the osteoclastic lineage. The greater osteoclast surface in $Y1^{-/-}$ mice, not evident in $Y2^{-/-}$, suggests that, although there is some evidence these receptors may share a common pathway to control osteoblastic activity, they differ in their ability to control cells of the osteoclast lineage. Importantly, this elevation in osteoclast indices was not sufficient to counteract the anabolic changes.

The similarity of osteoblast phenotypes between $Y1^{-/-}$ and $Y2^{-/-}$ mice suggested a common signaling pathway to regulate bone formation. In keeping with this, deletion of both the Y1 and Y2 receptors did not result in additive effects on bone mass. There were, however, some microarchitectural changes evident in these mice, with fewer, but thicker, trabeculae compared with single knockouts, which may relate to subtle shifts in the balance of resorption and formation. Consistent with this, the osteoclast surface was not elevated in $Y1^{-/-}Y2^{-/-}$ mice, suggesting a $Y2^{-/-}$-like phenotype. The dominance of the $Y2^{-/-}$ phenotype was not complete, however, with $Y1^{-/-}Y2^{-/-}$ mice showing a more $Y1^{-/-}$ like cortical bone phenotype. We previously showed that the effects of Y1 deletion to increase circulating insulin levels and enhance adiposity in mice were no longer evident when Y2 receptors were also missing (13), consistent with a dominant $Y2^{-/-}$-like effect on adipose homeostasis. Although Y1 and Y2 appear to share common pathways in the regulation of bone and adipose tissue, discreet actions of individual Y receptors are still apparent in these tissues.

In conclusion, this work provides clear evidence of a role for Y1 receptors in the regulation of skeletal homeostasis and indicates a direct role for these receptors to inhibit osteoblast activity. A peripheral site of action is supported by the lack of skeletal changes after hypothalamus-specific Y1 receptor deletion as well as the presence of Y1 receptors on osteoblasts and bone marrow stromal cells and the abolition of the effect of NPY on bone marrow stromal cells from Y1 receptor knock-out mice. Although these data also demonstrate that the hypothalamic Y1 receptors deleted in this study do not mediate the increased

adiposity observed in germ line Y1 receptor knock-out mice, they may play a role in modulating other feeding-related behaviors such as grinding and nesting, revealing an altered regulatory axis for the homeostatic and behavioral aspects of energy balance. The magnitude of changes evoked in bone and fat tissue by germ line loss of Y1 signaling suggests that targeting such pathways may represent effective therapeutic strategies for both skeletal fragility and obesity.

Acknowledgments—We thank Dr. Julie Ferguson (Biological Testing Facility, Garvan Institute of Medical Research), for facilitation of mouse studies, and Prof. Ulf Lerner, Dept. of Oral Cell Biology, Umeå University, for kindly providing access to the real-time PCR facility.

REFERENCES

1. Baldock, P. A., Sainsbury, A., Couzens, M., Enriquez, R. F., Thomas, G. P., Gardiner, E. M., and Herzog, H. (2002) *J. Clin. Invest.* **109,** 915–921
2. Sainsbury, A., Schwarzer, C., Couzens, M., Fetissov, S., Furtinger, S., Jenkins, A., Cox, H. M., Sperk, G., Hokfelt, T., and Herzog, H. (2002) *Proc. Natl. Acad. Sci. U. S. A.* **99,** 8938–8943
3. Sainsbury, A., Baldock, P. A., Schwarzer, C., Ueno, N., Enriquez, R. F., Couzens, M., Inui, A., Herzog, H., and Gardiner, E. M. (2003) *Mol. Cell Biol.* **23,** 5225–5233
4. Baldock, P. A., Thomas, G. P., Hodge, J. M., Baker, S. U., Dressel, U., O'Loughlin, P. D., Nicholson, G. C., Briffa, K. H., Eisman, J. A., and Gardiner, E. M. (2006) *J. Bone Miner. Res.* **21,** 1618–1626
5. Dumont, Y., Fournier, A., St-Pierre, S., Schwartz, T. W., and Quirion, R. (1990) *Eur. J. Pharmacol.* **191,** 501–503
6. Parker, R. M., and Herzog, H. (1999) *Eur. J. Neurosci.* **11,** 1431–1448
7. Wahlestedt, C., Grundemar, L., Hakanson, R., Heilig, M., Shen, G. H., Zukowska-Grojec, Z., and Reis, D. J. (1990) *Ann. N. Y. Acad. Sci.* **611,** 7–26
8. Morgan, D. G., Kulkarni, R. N., Hurley, J. D., Wang, Z. L., Wang, R. M., Ghatei, M. A., Karlsen, A. E., Bloom, S. R., and Smith, D. M. (1998) *Diabetologia.* **41,** 1482–1491
9. Iyengar, S., Li, D. L., and Simmons, R. M. (1999) *J. Pharmacol. Exp. Ther.* **289,** 1031–1040
10. Pedrazzini, T., Seydoux, J., Kunstner, P., Aubert, J. F., Grouzmann, E., Beermann, F., and Brunner, H. R. (1998) *Nat. Med.* **4,** 722–726
11. Pralong, F. P., Gonzales, C., Voirol, M. J., Palmiter, R. D., Brunner, H. R., Gaillard, R. C., Seydoux, J., and Pedrazzini, T. (2002) *FASEB J.* **16,** 712–714
12. Kushi, A., Sasai, H., Koizumi, H., Takeda, N., Yokoyama, M., and Nakamura, M. (1998) *Proc. Natl. Acad. Sci. U. S. A.* **95,** 15659–15664
13. Sainsbury, A., Bergen, H. T., Boey, D., Bamming, D., Cooney, G. J., Lin, S., Couzens, M., Stroth, N., Lee, N. J., Lindner, D., Singewald, N., Karl, T., Duffy, L., Enriquez, R., Slack, K., Sperk, G., and Herzog, H. (2006) *Diabetes* **55,** 19–26
14. Howell, O. W., Doyle, K., Goodman, J. H., Scharfman, H. E., Herzog, H., Pringle, A., Beck-Sickinger, A. G., and Gray, W. P. (2005) *J. Neurochem.* **93,** 560–570
15. Franklin, K. B., and Paxinos, G. (1997) *The Mouse Brain in Stereotaxic Coordinates*, Academic Press, San Diego
16. Baldock, P. A., Sainsbury, A., Allison, S., Lin, E. J., Couzens, M., Boey, D., Enriquez, R., During, M., Herzog, H., and Gardiner, E. M. (2005) *J. Bone Miner. Res.* **20,** 1851–1857
17. Gardiner, E. M., Baldock, P. A., Thomas, G. P., Sims, N. A., Henderson, N. K., Hollis, B., White, C. P., Sunn, K. L., Morrison, N. A., Walsh, W. R., and Eisman, J. A. (2000) *FASEB J.* **14,** 1908–1916
18. Siu, W. S., Qin, L., and Leung, K. S. (2003) *J. Bone Miner. Metab.* **21,** 316–322
19. Boonekamp, P. M., Hekkelman, J. W., Hamilton, J. W., Cohn, D. V., and Jilka, R. L. (1984) *Proc. Kon. Ned. Akad. Wetensch. Series B* **87,** 371–382
20. Cusin, I., Terrettaz, J., Rohner-Jeanrenaud, F., Zarjevski, N., Assimacopoulos-Jeannet, F., and Jeanrenaud, B. (1990) *Endocrinology* **127,** 3246–3248
21. Sainsbury, A., Rohner-Jeanrenaud, F., Cusin, I., Zakrzewska, K. E., Halban, P. A., Gaillard, R. C., and Jeanrenaud, B. (1997) *Diabetologia* **40,** 1269–1277
22. Standridge, M., Alemzadeh, R., Zemel, M., Koontz, J., and Moustaid-Moussa, N. (2000) *FASEB J.* **14,** 455–460
23. Moltz, J. H., and McDonald, J. K. (1985) *Peptides* **6,** 1155–1159
24. Sainsbury, A., Cusin, I., Rohner-Jeanrenaud, F., and Jeanrenaud, B. (1997) *Diabetes* **46,** 209–214
25. Baldock, P. A., Allison, S., McDonald, M. M., Sainsbury, A., Enriquez, R. F., Little, D. G., Eisman, J. A., Gardiner, E. M., and Herzog, H. (2006) *J. Bone Miner. Res.* **21,** 1600–1607
26. Sainsbury, A., Schwarzer, C., Couzens, M., and Herzog, H. (2002) *Diabetes* **51,** 3420–3427
27. Stephens, T. W., Basinski, M., Bristow, P. K., Bue-Valleskey, J. M., Burgett, S. G., Craft, L., Hale, J., Hoffmann, J., Hsiung, H. M., Kriauciunas, A., MacKellar, W., Rosteck, P. R., Jr., Schoner, B., Smith, D., Tinsley, F. C., Zhang, X.-Y., and Heiman, M. (1995) *Nature* **377,** 530–532
28. Campfield, L. A., Smith, F. J., Guisez, Y., Devos, R., and Burn, P. (1995) *Science* **269,** 546–549
29. Elefteriou, F., Takeda, S., Ebihara, K., Magre, J., Patano, N., Kim, C. A., Ogawa, Y., Liu, X., Ware, S. M., Craigen, W. J., Robert, J. J., Vinson, C., Nakao, K., Capeau, J., and Karsenty, G. (2004) *Proc. Natl. Acad. Sci. U. S. A.* **101,** 3258–3263
30. Pettersson, M., Ahren, B., Lundquist, I., Bottcher, G., and Sundler, F. (1987) *Cell Tissue Res.* **248,** 43–48
31. Koteja, P., Carter, P. A., Swallow, J. G., and Garland, T., Jr. (2003) *Physiol. Behav.* **80,** 375–383
32. Murzi, E., Baptista, T., and Hernandez, L. (1991) *Brain Res. Bull.* **26,** 321–325
33. Insel, T. R., and Harbaugh, C. R. (1989) *Physiol. Behav.* **45,** 1033–1041
34. Bjurholm, A., Kreicbergs, A., Schultzberg, M., and Lerner, U. H. (1988) *Acta Physiol. Scand.* **134,** 451–452
35. Bjurholm, A., Kreicbergs, A., Schultzberg, M., and Lerner, U. H. (1992) *J. Bone Miner. Res.* **7,** 1011–1019
36. Takeda, S., Elefteriou, F., Levasseur, R., Liu, X., Zhao, L., Parker, K. L., Armstrong, D., Ducy, P., and Karsenty, G. (2002) *Cell* **111,** 305–317
37. Kalariti, N., and Koutsilieris, M. (2004) *In Vivo* **18,** 621–628
38. Ofek, O., Karsak, M., Leclerc, N., Fogel, M., Frenkel, B., Wright, K., Tam, J., Attar-Namdar, M., Kram, V., Shohami, E., Mechoulam, R., Zimmer, A., and Bab, I. (2006) *Proc. Natl. Acad. Sci. U. S. A.* **103,** 696–701
39. Lundberg, P., Allison, S. J., Lee, N., Baldock, P. A., Brouard, N., Rost, S., Enriquez, R., Sainsbury, A., Lamghari, M., Simmons, P., Eisman, J. A., Gardiner, E. M., and Herzog, H. (2007) *J. Biol. Chem.* **282,** 19082–19091